Amyloid β peptide-dependent activation of human platelets: essential role of Ca^{2+} and ADP in aggregation and thrombus formation

Ilaria Canobbio[1], Gianni F. Guidetti[1], Barbara Oliviero[2], Daria Manganaro[1], *Mauro Torti[1], *Giordano Pula[3]

1 Department of Biology and Biotechnology, Unit of Biochemistry, University of Pavia, Pavia
2 Department of Infectious Diseases, Fondazione Istituto di Ricovero e Cura a Carattere Scientifico Policlinico San Matteo, Pavia, Italy
3 Department of Pharmacy and Pharmacology, University of Bath, Bath, UK

*M.T. and G.P. are co-senior authors

Running title: ***Amyloid β peptide activates platelets through ADP release***

To whom correspondence should be addressed: Ilaria Canobbio, Department of Biology and Biotechnology, Unit of Biochemistry, University of Pavia, via Bassi 21, Pavia; Tel: +39 0382 987243; Fax +39 0382 987240; e-mail: ilaria.canobbio@unipv.it

Keywords: ADP, Amyloid, Alzheimer's disease, Ca^{2+}, Platelets, Secretion, Thrombosis

Background: Alzheimer's disease impairs brain circulation by inducing blood clotting.

Results: Amyloid β peptide in Alzheimer's brain tissue increases platelet intracellular Ca^{2+}, dense granule secretion and ADP release.

Conclusion: Amyloid β peptide induces blood clotting by directly activating platelets.

Significance: This study explains the link between Alzheimer's disease and poor brain blood supply and suggests new treatments for this disease.

ABSTRACT

Alzheimer's disease is a highly debilitating disease of the central nervous system associated with the accumulation of amyloid β (Aβ) peptides in the brain. Besides their cytotoxic effect on neurons, Aβ peptides are thought to be responsible for the atherothrombotic complications associated with Alzheimer's disease, which are collectively known as cerebrovascular disease. In this study, we have investigated the effect of Aβ peptides on human platelet signal transduction and function. Using live cell Ca^{2+} spectrofluorimetry, we discovered that Aβ peptides induce an increase in platelet intracellular Ca^{2+} similar to physiological agonists. This increase of intracellular Ca^{2+} stimulates α- and dense granules secretion and leads to the release of the secondary agonist ADP. Released ADP acts in an autocrine manner as a stimulant for critical signaling pathways leading to the activation of platelets, which include the activation of the protein kinases Syk, protein kinase C, Akt, and mitogen-activated protein kinases. Ca^{2+}-dependent release of ADP is also responsible for the activation of the small GTPase Rap1b and the fibrinogen receptor integrin αIIbβ3, which leads to increased platelet aggregation and increased thrombus formation in human whole blood. Our discoveries complement existing understanding of the role of Aβ peptides in cerebrovascular dementia and suggest the inhibition of ADP signaling as a potential therapeutic avenue in the treatment of Alzheimer's disease.

INTRODUCTION

Abnormal metabolism of the amyloid precursor protein (APP) through the amyloidogenic pathway results in the accumulation of heterogeneous amyloid β (Aβ) peptides (40-42 amino acids) in the central nervous system, causing the onset of Alzheimer's disease (AD) (1,2). Amyloid peptides accumulate also in the cerebrovascular

system of AD patients and play a role in the onset and progression of cerebrovascular diseases, such as stroke and cerebral amyloid angiopathy (CAA) (3). Amyloid Aβ peptides are responsible for the prothrombotic state described in several AD patients, where increased clot formation, decreased fibrinolysis, and elevated levels of coagulation factors are responsible for reduced blood flow to the brain, neuroinflammation and ultimately neurodegeneration (4). Platelets are the major source of amyloid peptides found in plasma. Platelets express the amyloid precursor protein APP and the enzymatic machinery responsible for its metabolism and for the generation of Aβ peptides (5-7). In physiological conditions platelets metabolize APP through the *non-amyloidogenic* pathway: α-secretase is activated by Ca^{2+} and calmodulin (8) and releases soluble APPα (sAPPα) which regulates thrombosis and hemostasis in vivo (9). In AD, however, β– and γ-secretases activity increases, and APP is metabolized to produce amyloid β peptides, which leads to alteration of the APP content of platelets (10). Soluble APP fragments and Aβ peptides are stored in platelet α–granules and released upon stimulation with physiological agonists (11). Several studies suggested that platelet-derived Aβ peptides may represent a reliable peripheral biomarker of AD (12,13). Abnormalities in platelet membrane fluidity and secretase activity, as well as increased APP level have been documented in platelets from AD patients (14).

It has become increasingly clear that Aβ peptides directly activate platelets. Herczenik and coworkers showed that misfolded amyloid peptides induce platelet activation and aggregation through two different pathways initiated by CD36 or GPIb, respectively (15). A short peptide corresponding to the biologically active sequence of Aβ ($Aβ_{25-35}$) (16,17) is able to activate human platelets and potentiate platelet aggregation induced by low doses of collagen, ADP and thrombin through phosphoinositide 3-kinase (PI3K) and p38 mitogen-activated protein kinase (MAPK)-dependent pathway (18,19). Sonkar et al. have recently demonstrated that $Aβ_{25-35}$ stimulates platelet activation through RhoA dependent modulation of actomyosin organization (20). Moreover, immobilized Aβ peptides are able to induce platelet adhesion and activation of intracellular signaling pathway, and to fasten spreading over collagen (21). Despite these reports, the exact mechanism responsible for Aβ peptides-dependent activation of platelets remains elusive.

In the present study, we investigated further the molecular mechanism of Aβ-induced platelet activation. One of the most interesting hypotheses on the mechanism for Aβ toxicity is based on the ability of the peptides to form cation permeable pores in the cellular membranes, which ultimately results in membrane depolarization, Ca^{2+} leakage, and disruption of ionic homeostasis (22,23). Because of the effect of Aβ peptides on intracellular Ca^{2+} in other cell types (24), we investigated the effect of this protein on platelet intracellular Ca^{2+} homeostasis. We demonstrated that Aβ peptides are directly responsible for Ca^{2+} mobilization and granule secretion. The resulting release of ADP stimulates canonical signaling pathways, leading to activation of protein kinase C (PKC), PI3K, mitogen-activated protein kinases p38MAPK and extracellular signal-regulated kinase (ERK) as well as tyrosine kinases. These events support platelet aggregation and thrombus formation in human whole blood under physiological shear stress. Taken together, our data unequivocally identify Ca^{2+}-dependent release of ADP as the molecular mechanism underlying the pro-thrombotic effect of Aβ peptides and further clarifies the link between AD and cerebrovascular disease.

EXPERIMENTAL PROCEDURES

Materials

$Aβ_{25-35}$, bovine serum albumin (BSA), dimethylsulfoxide (DMSO), prostaglandin E_1, indomethacin, apyrase grade I and VII, collagen type I, leupeptin, aprotinin; BAPTA and calcein AM (green) were purchased from Sigma-Aldrich (Milan, Italy). The rabbit polyclonal Abs against Rap1 (121), Syk (N19) and the mAb anti-tubulin (DM1A) were from Santa Cruz Biotechnology (Santa Cruz, US). Anti- phospho-Akt(S473), anti-phospho-p38MAPK(T180/Y182), anti-phospho-ERK1/2(T202/Y204), anti-phospho-MLC(S19), and anti-PKC phospho-substrates were from Cell Signaling Technology (Danvers, US). Appropriate peroxidase-conjugated anti-IgG Abs were from Bio-Rad. The enhanced

chemiluminescence (ECL) substrate and Fura 2-AM were from Millipore (Vimodrone, Italy). FITC-labeled fibrinogen was from Molecular Probes (Eugene, US). FITC-conjugated human P-selectin was from Beckman Coulter (Pasadena, US). ATP determination kit was from Biaffin (Kasser, Germany).

Preparation of washed human platelets

Human platelets were obtained from healthy volunteers essentially as previously described with minor modifications (25). Briefly, whole blood in citric acid/citrate/dextrose (152 mM sodium citrate, 130 mM citric acid, 112 mM glucose) was centrifuged at 120 × *g* for 10 min at room temperature. Apyrase grade I (0.2 units/ml), prostaglandin E_1 (1 μM), and indomethacin (10 μM) were then added to the platelet-rich plasma (PRP). Platelets were recovered by centrifugation at 720 × *g* for 15 min, washed with 10 ml of PIPES buffer (20 mM PIPES, 136 mM NaCl, pH 6.5), and finally gently resuspended in HEPES buffer (10 mM HEPES, 137 mM NaCl, 2.9 mM KCl, 12 mM $NaHCO_3$, pH 7.4). The cell count was typically adjusted to 5×10^8 platelets/ml unless otherwise stated.

Analysis of platelet activation

Unless differently stated, platelet samples were typically stimulated with 10-20 μM $A\beta_{25\text{-}35}$ or 0.1 U/ml thrombin as a control. Aggregation of platelets (2×10^8 platelets/ml, 0.25 ml) was monitored continuously in a Born lumiaggregometer up to 5 minutes. Rap1b activation was analyzed by a pull down assay using the GST-tagged Rap-binding domain of RalGDS (GST–RalGDSRBD) essentially as described previously, and precipitated active Rap1b was identified by immunoblotting with an anti-Rap1 antibody (26). Measurement of cytosolic Ca^{2+} was performed on 0.4 ml samples of Fura-2AM-loaded platelets under gentle stirring in a PerkinElmer Life Sciences LS3 spectrofluorimeter in the presence of 1mM $CaCl_2$, or 2mM EGTA, according to a previously published procedure (27). For analysis of protein phosphorylation, identical amounts of proteins from whole platelet lysates were separated by SDS-PAGE on 5-15% or 10-20% acrylamide gradient gels, and transferred to PVDF. Immunoblotting analysis was performed as previously described (28), using the following antibodies and dilutions: anti-Syk (N-19); anti-phospho-Akt (S473), anti-phospho-p38MAPK (T180/Y182), anti-phospho-ERK1/2 (T202/Y204), and anti-phospho-MLC (S19):1:500; anti-PKC phospho-substrates, anti-tubulin (DM1A), and anti-Rap1 (121): 1:1000. Reactive proteins were visualized with a chemiluminescence reaction. All of the immunoblots are representative of at least 3 different experiments giving similar results.

Flow cytometry

Samples of washed platelets (10^6 cells in 0.05 ml of HEPES buffer containing 1 mM $CaCl_2$ and 1 mM $MgCl_2$ and 0.2% BSA), untreated or activated with different doses of $A\beta_{25\text{-}35}$ were labeled for 10 minutes at room temperature with different specific antibodies: Fluorescein isothiocyanate (FITC)-conjugated anti-P-selectin, or FITC-conjugated fibrinogen. Reaction was stopped by diluting samples with 0.45 ml HEPES buffer. Samples were immediately analyzed by flow cytometry using a FACSCalibur instrument equipped with CellQuest Pro software (BD Bioscience, Milan Italy). Data analyses were performed using FlowJo 7.6.1 software (Tree Star Inc., Ashland, US).

Measurement of [^{14}C]serotonin secretion and ATP/ADP release

Agonist-induced release of [^{14}C]serotonin from metabolically labeled platelets was performed as previously described (27). Platelet secretion was determined by measuring the release of ATP by adding luciferin-luciferase reagent. Briefly, 5×10^8/ml (0.3ml) were stimulated with the indicated concentrations of $A\beta_{25\text{-}35}$, and reactions were stopped by adding 10mM EDTA. Cells were spun down and 50 μl of supernatant were analyzed with the ATP determination kit (Biaffin, Kasser, Germany) following manufacture's instruction.

Thrombus formation assay

The Bioflux200 system (Fluxion, South San Francisco, US) was used to analyze thrombus formation in human whole blood under flow essentially as previously described (29). Microchannels were coated 30 minutes with 1mg/ml collagen I (monomeric collagen from calf skin), before blocking with 0.5% bovine serum albumin and washing with modified Tyrode's buffer. Platelet-rich plasma (PRP) was isolated from blood by centrifugation

(200×g, 15 min) and incubated for 1 hour with Calcein™ (5μg/ml) at 37°C to facilitate thrombus visualization in whole blood. PRP was then added to the red blood cell fraction to reconstitute whole blood with physiological blood cell density (including platelets) and thrombus formation (on collagen) were visualized by fluorescence microscopy. Where indicated, 20 μM $A\beta_{25-35}$ and/or 2U/ml apyrase was added to PRP 10 minutes before the start of the flow assay. Platelet adhesion under flow conditions was tested on collagen I (shear rate = 1000 sec^{-1}). Representative pictures were taken at time 10 minutes and surface area coverage was measured using Bioflux200 Software (version 2.4).

Statistical analysis

Data are expressed throughout as mean ± SEM. The results were analyzed by t-test (for comparisons of two groups) or one-way ANOVA with Bonferroni post-test (for multiple comparisons).

RESULTS

$A\beta_{25-35}$ induces intracellular Ca^{2+} increase and granule release

Several studies demonstrate that the toxicity of Aβ peptides resides in the ability to form cation pores permeable to Ca^{2+}, which causes membrane depolarization (22). The ability of forming ionic pores has been demonstrated for amyloid peptides of different length, including the short $A\beta_{25-35}$ peptide (30). Notably, the $A\beta_{25-35}$ is regarded as the functional domain responsible for the neurotoxic properties of Aβ peptides, of which it represents the biologically active region (16). Therefore $A\beta_{25-35}$ has been widely used to investigate the biological properties of Aβ peptides in different cell types including platelets (18-21).

In this study, we analyzed the direct effect of $A\beta_{25-35}$ on Ca^{2+} mobilization in washed human platelets labeled with Fura-2AM, both in the presence and in the absence of extracellular Ca^{2+}. Representative traces reported in Figure 1A show platelet Ca^{2+} movements in the presence of 1mM extracellular $CaCl_2$ upon stimulation with thrombin or $A\beta_{25-35}$. 20μM $A\beta_{25-35}$ induces a slow increase in Ca^{2+} with a kinetic profile different from the spike observed in thrombin-stimulated platelets. Pretreatment of platelets with EGTA, which chelates extracellular Ca^{2+}, completely abolishes Ca^{2+} movements. Quantitative analysis shown in Figure 1B reveals that $A\beta_{25-35}$ promotes a statistically significant increase in intracellular Ca^{2+}. Recent evidence suggested a pivotal role for RhoA in platelet activation induced by $A\beta_{25-35}$ and the activity of Rho-associated coiled-coil protein kinase (ROCK) was found necessary for $A\beta_{25-35}$-induced cytoskeletal rearrangements and aggregation (20). Therefore, we tested the effect of the ROCK inhibitor Y27632 on $A\beta_{25-35}$-induced increase in intracellular Ca^{2+} and demonstrated that Ca^{2+} influx is upstream of RhoA activation in the signaling event stimulated by $A\beta_{25-35}$ (Figure 1C). In addition, pre-incubation of platelets with the ADP-degrading enzyme apyrase does not significantly affect intracellular Ca^{2+} movements induced by $A\beta_{25-35}$, suggesting that this effect of $A\beta_{25-35}$ is not ADP-dependent (Figure 1C).

Platelet granule secretion was next analyzed. In the presence of 1mM $CaCl_2$ $A\beta_{25-35}$ induces a dose-dependent α-granule release, measured as P-selectin exposure, and dense granules release, measured as ^{14}C-serotonin secretion (Figure 2). Dense granule secretion is significantly reduced in the absence of extracellular $CaCl_2$ suggesting that $A\beta_{25-35}$-induced Ca^{2+} influx in platelets is required for dense granule release. Platelet dense granule release was also evaluated by measuring the extracellular accumulation of ADP/ATP using the luciferin/luciferase assay. We found that platelets at the physiological density of 5 x 10^8/ml release ADP at the concentration of 0.146 ± 0.1 and 0.184 ± 0.13 μM in response to 10 μM and 20 μM $A\beta_{25-35}$, respectively.

$A\beta_{25-35}$ stimulates activatory signaling pathways in an ADP-dependent manner

It has been demonstrated that $A\beta_{25-35}$ is able to activate intracellular signaling pathways initiating a cascade of phosphorylation of different effectors, namely mitogen activated protein kinases p38MAPK and ERK1/2, PI3K and PKC (18,19). In light of the ability of $A\beta_{25-35}$ to promote granule secretion and ADP release, we investigated the possible role of ADP in platelet activation induced by $A\beta_{25-35}$.

Immunoblotting analysis with phospho-specific antibodies shows that $A\beta_{25-35}$ induces a time-dependent phosphorylation of several key signaling proteins. These substrates include the MAPKs p38MAPK and ERK1/2, the PI3K-regulated kinase Akt, and the PKC substrate pleckstrin (Figure 3A). Moreover, $A\beta_{25-35}$ promotes the rapid and robust tyrosine phosphorylation of several proteins as identified using the phosphotyrosine-specific antibody 4G10 (Figure 3B). Phospho-specific bands in Figure 3B include a substrate with an apparent molecular mass of about 70 kDa, which is likely to be the non-receptor tyrosine kinase Syk. In fact, the $A\beta_{25-35}$-dependent phosphorylation of Syk has been confirmed by immunoprecipitation experiments (Figure 3C). Interestingly, $A\beta_{25-35}$-induced phosphorylation of these substrates is completely prevented in the presence of the ADP scavenger apyrase, indicating that the positive signaling initiated by secreted ADP plays a critical role in $A\beta_{25-35}$-induced platelet activation. Accordingly to previous evidence (20), $A\beta_{25-35}$ also induces phosphorylation of the Ca^{2+}-regulated myosin light chain (MLC), which, however, is only partially reduced by pre-incubation of platelets with apyrase (Figure 3D), suggesting that, in contrast to the molecular events described above, MLC phosphorylation is at least partially promoted in an ADP- and granule secretion-independent manner.

Flow cytometry analysis of FITC-labelled fibrinogen binding to platelets demonstrates that $A\beta_{25-35}$ stimulates integrin αIIbβ3 inside-out activation in a concentration-dependent manner (Figure 4). Next we analyzed the activation of the small GTPase Rap1b, which is an essential regulator of integrin inside-out signaling (31,32). Using a pull down assay we demonstrated that $A\beta_{25-35}$ dose dependently stimulates Rap1b activation (Figure 5A). Accumulation of Rap1b-GTP by $A\beta_{25-35}$ is rapid but transient, as it reverts after 1 minute (Figure 5B). Remarkably, the activation of Rap1b by $A\beta_{25-35}$ is independent of integrin αIIbβ3 since it is not modified by pre-incubation with RGDS, but it is completely abolished in the presence of apyrase (Figure 5C), suggesting that the release of ADP is the molecular mechanism underlying the regulation of this GTPase by $A\beta_{25-35}$.

Endogenous ADP release is necessary for $A\beta_{25-35}$-induced platelet aggregation and increase thrombus formation under flow

We next analyzed the ability of $A\beta_{25-35}$ to stimulate platelet aggregation and investigated its mechanism of action. Platelet aggregation was induced by different concentrations of $A\beta_{25-35}$ under constant stirring in a Born lumiaggregometer in the presence of 1 mM extracellular Ca^{2+} (Figure 6A). $A\beta_{25-35}$ dose dependently induces platelet aggregation. $A\beta_{25-35}$-induced aggregation is mediated by integrin activation since it is blocked by treatment with RGDS peptide (data not shown) and depends on Ca^{2+} as it is strongly reduced in the absence of extracellular Ca^{2+} and by preincubation with intracellular Ca^{2+} chelator BAPTA (Figure 6B). The role of $A\beta_{25-35}$-induced ADP secretion was tested using the ADP degrading enzyme apyrase, which strongly reduces platelet aggregation induced by $A\beta_{25-35}$ (Figure 6C). As a control, we assessed the release of α- and dense granules in the presence of apyrase (Figure 6D and E, respectively). Neither were affected by apyrase, suggesting that the regulation of platelet degranulation is upstream of the effect on platelet aggregation.

We have previously demonstrated that platelets are able to adhere on immobilized Aβ peptides in static condition and to fasten spreading over collagen (21). Here, we evaluated the ability of $A\beta_{25-35}$ to potentiate platelet adhesion to collagen and thrombus formation under physiological flow conditions. Platelets from human whole blood were selectively labelled with calcein AM and the formation of thrombi under arterial shear stress (1000 sec^{-1}) was assessed as previously described (29). As shown in Figure 7A, platelet adhesion and thrombus formation on collagen-coated surfaces is significantly increased by collagen co-incubation with 10μM $A\beta_{25-35}$ during coating. Surprisingly, addition of $A\beta_{25-35}$ directly to blood does not increase thrombus adhesion on collagen-coated surfaces (data not shown), possibly due to increased platelet-platelet interaction rather than potentiation of adhesion to absorbed collagen. Pre-treatments of platelets with apyrase ablates the increase in thrombus formation observed in our experiments (Figure 7B), which further suggests the

importance of ADP release in the potentiatory effect of $A\beta_{25-35}$.

DISCUSSION

The ability of Aβ peptides to promote activation and adhesion of platelets has been previously reported by our group and others (18-21), and is likely to significantly contribute to the development and progression of cerebrovascular diseases associated with AD. In the present study, we investigated the molecular mechanism underlying the activation of platelets by Aβ peptides, and we demonstrated for the first time the crucial and hierarchical role of intracellular Ca^{2+} increase and ADP secretion. We propose that Ca^{2+}-mediated dense granule release and secretion of ADP is an early event in platelet stimulation by $A\beta_{25-35}$, and that secreted ADP is the major player in the stimulation and propagation of platelet activation. We demonstrated that pre-incubation of platelets with ADP scavenging enzyme apyrase strongly reduce $A\beta_{25-35}$-induced platelet aggregation and potentiation of thrombus formation. Activation of the small GTPase Rap1b and consequentially integrin $\alpha_{IIb}\beta_3$ stimulation, are also dependent on ADP. Moreover, $A\beta_{25-35}$-induced phosphorylation and activation of signaling protein Syk, PKC, PI3K, and mitogen activated kinases p38MAPK and ERK1/2 dependent on ADP, since are completely abolished in the presence of apyrase. Our current data reinforce our previous studies showing that although static platelet adhesion to immobilized Aβ peptides is not dependent on ADP, even in these conditions the release of ADP reinforces the activation of intracellular signaling pathways (21).

In our experiments, we detected a slow and significant increase of the intracellular Ca^{2+} concentration in platelets treated with $A\beta_{25-35}$ peptide, a widely used tool representing the biologically active portion of both the naturally generated fibrillogenic peptide $A\beta_{1-40}$ and $A\beta_{1-42}$ peptides (16). Our data clearly show that $A\beta_{25-35}$ induces a significant increase in intracellular Ca^{2+}, which is necessary for the stimulation of $A\beta_{25-35}$-induced α- and dense granule release, and is critical for platelet aggregation. This observation is consistent with previous hypotheses that Aβ peptides can generate pores in the plasma membrane of cells leading to Ca^{2+} influx from the extracellular space (22-23;33). However, it remains unclear, at the present, whether $A\beta_{25-35}$ generates pores in the plasma membrane of human platelets to allow Ca^{2+} influx or whether it regulates pre-existing Ca^{2+} channel. Hence, the molecular mechanisms linking Aβ peptides to platelet intracellular Ca^{2+} increase remains elusive and will require further investigation.

We documented the activation of PKC in $A\beta_{25-35}$-stimulated platelets, as revealed by the phosphorylation analysis of the intracellular protein pleckstrin (34). The activation of PKC (which is usually downstream of PLC activation, IP3 generation and release of Ca^{2+} from intracellular stores, 35) is not an early event in platelet activation by Aβ peptide. In fact, differently to what we observed for the intracellular Ca^{2+} increase, the complete inhibition of pleckstrin phosphorylation by the ADP scavenger apyrase demonstrates that PLC/PKC activation is secondary to granule release. These observations are in partial disagreement with a previous study indicating that inhibition of PKC by Ro318220 prevents $A\beta_{25-35}$-induced Ca^{2+} increase (19). Although it is difficult to understand the reason for this discrepancy, we would like to highlight that the inhibition of the Ca^{2+} spike shown by those authors is only partial, which is not excluding the possibility of a double source for the intracellular Ca^{2+} increase in response to $A\beta_{25-35}$ (i.e. partially from membrane permeabilization and partially from intracellular store release). Moreover, the limited specificity of Ro318220 could be responsible for some misinterpretation of the data in the above study (36).

Recently, an important early role for the RhoA-activated protein kinase ROCK in platelet activation by $A\beta_{25-35}$ has been proposed (20). Although the ROCK inhibitor Y27632 did not inhibit the Ca^{2+} wave induced by Aβ peptides, our data presented here are not in disagreement with this publication. In fact, although we prove that ROCK is not responsible for the initial increase in intracellular Ca^{2+}, our data do not exclude that ROCK is indeed stimulated by Aβ peptides and plays an important role in the resulting platelet activation. This is in agreement with our data showing that MLC (a known substrate for ROCK) is phosphorylated in response to platelet incubation with $A\beta_{25-35}$.

One of the strengths of our data is in the identification of a strong intracellular Ca^{2+}-

dependent stimulation of granules secretion in the presence of Aβ peptides. Interestingly, upon stimulation with Aβ peptides, MLC is rapidly phosphorylated, which is likely to result in the reorganization of actomyosin contractility and the release of α- and dense granules (37). Interestingly, the inhibition of ADP in our cell signaling experiments completely abolished the phosphorylation of all intracellular targets analyzed yet it only marginally reduced the phosphorylation of MLC, suggesting that this cellular event occurs upstream of granule secretion, and may be directly driven by intracellular Ca^{2+} increase. On the other hand, the activation of the other protein kinases investigated herein and their signaling is likely to be a consequence of granule and ADP release.

Taken together, our data suggest the centrality of ADP in the stimulation of platelet activation, aggregation and thrombus formation by Aβ peptides. As shown in figure 8, we propose a signaling model for Aβ peptides stimulation of platelet responses, in which extracellular Ca^{2+} influx into the platelet leads to dense granules release and ADP secretion, and consequent ADP-dependent signaling through several intracellular protein kinase pathways and activation of Rap1b. As previously shown (38), the activation of Rap1b leads to integrin inside-out signaling and stimulates fibrinogen binding at the base of key physiological phenomena such as platelet aggregation and thrombus formation. To our knowledge, our novel observations clarify the pathological role of Aβ peptides in cerebrovascular disease and indicate that platelet ADP receptors are novel targets for the treatment of vascular complications of AD.

REFERENCES

1.Hardy, J.A., Higgins, G.A. (1992) Alzheimer's disease: the amyloid cascade hypothesis. *Science*. **256**,184-185

2.Gandy, S. (2005) The role of cerebral amyloid beta accumulation in common forms of Alzheimer disease. *J Clin Invest.* **115**:1121-1129.

3. Viswanathan, A., Greenberg, S.M. (2011) Cerebral amyloid angiopathy in the elderly. *Ann Neurol.* **70**, 871-880

4. Cortes-Canteli, M., Zamolodchikov, D., Ahn, H.J., Strickland, S., Norris, E.H. (2012) Fibrinogen and altered hemostasis in Alzheimer's disease. *J Alzheimers Dis.***32**,599-608.

5. Van Nostrand, W.E., Schmaier, A.H., Farrow, J.S., Cunningham, D.D. (1990) Protease nexin-II (amyloid beta-protein precursor): a platelet alpha-granule protein. *Science.* **248**, 745-748

6. Tang, K., Hynan, L,.S., Baskin, F., Rosenberg, R.N. (2006) Platelet amyloid precursor protein processing: a bio-marker for Alzheimer's disease. *J Neurol Sci.* **240**, 53-58

7. Catricalà, S., Torti, M., Ricevuti, G. (2012) Alzheimer disease and platelets: how's that relevant. *Immun Ageing*. **9**, 20-27

8. Canobbio, I., Catricalà, S., Balduini, C., Torti, M. (2011) Calmodulin regulates the non-amyloidogenic metabolism of amyloid precursor protein in platelets. *Biochim Biophys Acta.* **1813**, 500-506

9. Xu, F., Previti, M.L., Nieman, M.T., Davis, J., Schmaier, A.H., Van Nostrand,W.E. (2009) AbetaPP/APLP2 family of Kunitz serine proteinase inhibitors regulate cerebral thrombosis. *J Neurosci.* **29**, 5666-5670

10. Zainaghi, I.A., Talib, L.L., Diniz, B.S., Gattaz, W.F., Forlenza, O.V. (2012) Reduced platelet amyloid precursor protein ratio (APP ratio) predicts conversion from mild cognitive impairment to Alzheimer's disease. *J Neural Transm.* **119**:815-819

11. Li, Q.X., Berndt, M.C., Bush, A.I., Rumble, B., Mackenzie, I., Friedhuber, A., Beyreuther, K., Masters, C.L. (1994) Membrane-associated forms of the beta A4 amyloid protein precursor of Alzheimer's disease in human platelet and brain: surface expression on the activated human platelet. *Blood.***84**, 133-142

12. Evin, G., Li, Q.X. (2012) Platelets and Alzheimer's disease: Potential of APP as a biomarker. *World J. Psychiatry.* **2**,102-113

13. Jelic, V., Hagman, G., Yamamoto, N.G., Teranishi, Y., Nishimura, T., Winblad, B., Pavlov,P.F. (2013). Abnormal platelet amyloid-β protein precursor (AβPP) metabolism in Alzheimer's disease: identification and characterization of a new AβPP isoform as potential biomarker. *J Alzheimers Dis*.**35**,285-295.

14. Vignini, A., Morganti, S., Salvolini, E., Sartini, D., Luzzi, S., Fiorini, R., Provinciali, L., Di Primio, R., Mazzanti, L., Emanuelli, M. (2013) Amyloid precursor protein expression is enhanced in human platelets from subjects with Alzheimer's disease and frontotemporal lobar degeneration: a real-time PCR study. *Exp. Gerontol.* **48**,1505-1508.

15. Herczenik, E., Bouma, B., Korporaal, S.J., Strangi, R., Zeng, Q., Gros, P., Van Eck, M., Van Berkel, T.J., Gebbink, M.F., Akkerman, J.W. (2007) Activation of human platelets by misfolded proteins. *Arterioscler. Thromb. Vasc. Biol.* **27**, 1657-1665.

16. Kaminsky, Y.G., Marlatt, M.W., Smith, M.A., Kosenko, E.A. (2010) Subcellular and metabolic examination of amyloid-beta peptides in Alzheimer disease pathogenesis: evidence for Abeta(25-35). *Exp. Neurol*. **221**, 26-37

17. Millucci, L., Ghezzi, L., Bernardini, G., Santucci, A. (2010) Conformations and biological activities of amyloid beta peptide 25-35. *Curr Protein Pept Sci.* **11**,54-67

18. Shen, M.Y., Hsiao, G., Fong, T.H., Chen, H.M., Chou, D.S., Lin, C.H., Sheu, J.R., Hsu, C.Y. (2008) Amyloid beta peptide-activated signal pathways in human platelets. *Eur J Pharmacol.* **588**, 259-266

19. Shen, M.Y., Hsiao, G., Fong ,T.H., Chou, D.S., Sheu, J.R. (2008) Expression of amyloid beta peptide in human platelets: pivotal role of the phospholipase Cgamma2-protein kinase C pathway in platelet activation. *Pharmacol. Res.* **57**, 151-158

20. Sonkar, V.K., Kulkarni, P.P., Dash, D. (Jan 13, 2014) Amyloid β peptide stimulates platelet activation through RhoA-dependent modulation of actomyosin organization. *FASEB J.* PubMed PMID: 24421399

21. Canobbio, I. , Catricalà, S., Di Pasqua, L.G., Guidetti, G., Consonni, A., Manganaro, D., Torti, M. (2013). Immobilized amyloid Aβ peptides support platelet adhesion and activation. *FEBS Lett.* **587**:2606-2611

22. Pollard, H.B., Arispe, N., Rojas, E. Ion channel hypothesis for Alzheimer amyloid peptide neurotoxicity (1995). *Cell Mol Neurobiol.* **15**, 513-26

23. Demuro, A., Parker, I., Stutzmann, G.E. (2010) Calcium signaling and amyloid toxicity in Alzheimer disease. *J Biol Chem.* **285**, 12463-12468

24. Mattson, M.P., Goodman, Y. (1995) Different amyloidogenic peptides share a similar mechanism of neurotoxicity involving reactive oxygen species and calcium. *Brain Res.* **676**, 219-224

25. Canobbio, I., Reineri, S., Sinigaglia, F., Balduini, C., Torti, M. (2004) A role for p38 MAPkinase in platelet activation by von Willebrand factor. *Thromb Haemost.* **91**,102-110

26. Guidetti GF, Manganaro D, Consonni A, Canobbio I, Balduini C, Torti M.(2013) Phosphorylation of the guanine-nucleotide-exchange factor CalDAG-GEFI by protein kinase A regulates Ca(2+)-dependent activation of platelet Rap1b GTPase. *Biochem J*. **453**:115-123

27. Lova P, Guidetti GF, Canobbio I, Catricalà S, Balduini C, Torti M. (2011) Epinephrine-mediated protein kinase C and Rap1b activation requires the co-stimulation of Gz-, Gq-, and Gi-coupled receptors. *Thromb Haemost.* **105**:479-486

28. Canobbio, I., Cipolla, L., Consonni, A., Momi, S., Guidetti, G., Oliviero, B., Falasca, M., Okigaki, M., Balduini, C., Gresele, P., Torti, M. (2013) Impaired thrombin-induced plateletactivation and thrombus formation in mice lacking the Ca(2+)-dependent tyrosine kinase Pyk2. *Blood.* **121**, 648-657

29. Vara, D., Campanella, M., Pula, G. (2013) The novel NOX inhibitor 2-acetylphenothiazineimpairs collagen-dependent thrombus formation in a GPVI-dependent manner. *Br J Pharmacol.* **168**, 212-224

30. Engstrom, I., Ronquist, G., Petterssonm, L., Waldenström, A. (1995) Alzheimer amyloid beta-peptides exhibit ionophore-like properties in human erythrocytes. *Eur J Clin Invest.* **25**,471-476.

31. Guidetti, G.F., Torti, M. (2012) The Small GTPase Rap1b: A Bidirectional Regulator of Platelet Adhesion Receptors. *J Signal Transduct.* **2012**:412089.

32. Torti, M., Bertoni, A., Canobbio, I., Sinigaglia, F., Lapetina, E.G., Balduini, C. (1999) Rap1Band Rap2B translocation to the cytoskeleton by von Willebrand factor involve FcgammaII receptor-mediated protein tyrosine phosphorylation. *J Biol Chem.* **274**, 13690-13697

33. Kagan, B.L. (2012) Membrane pores in the pathogenesis of neurodegenerative disease. *Prog Mol Biol Transl Sci*. **107**,295-325

34. Lian, L., Wang, Y., Flick, M., Choi, J., Scott, E.W., Degen, J., Lemmon, M.A., Abrams, C.S. (2009) Loss of pleckstrin defines a novel pathway for PKC-mediated exocytosis. *Blood.* **113**,3577-3584

35. Oancea, E., Meyer, T. (1998) Protein kinase C as a molecular machine for decoding calcium and diacylglycerol signals. *Cell* **95**, 307–18

36. Davies, S.P., Reddy, H., Caivano, M., Cohen P. (2000) Specificity and mechanism of action of some commonly used protein kinase inhibitors. *Biochem J.* **351**, 95-105

37. Getz, T.M., Dangelmaier, C.A., Jin, J., Daniel, J.L., Kunapuli, S.P. (2010) Differential phosphorylation of myosin light chain (Thr)18 and (Ser)19 and functional implications in platelets. *J Thromb Haemost*. **8**, 2283-2289

38. Bertoni, A., Tadokoro, S., Eto, K., Pampori, N., Parise, L.V., White, G.C., Shattil, S.J.(2002) Relationships between Rap1b, affinity modulation of integrin alpha IIbbeta 3, and the actin cytoskeleton. *J Biol Chem.* **277**, 25715-25721

FIGURE LEGENDS

Figure 1. $A\beta_{25-35}$ induces Ca^{2+} inward in washed platelets

Platelets (2×10^8/ml, 0.4ml) were loaded with Fura-2AM (3μM, 40 minutes) and stimulated with 1U/ml thrombin or 20μM $A\beta_{25-35}$ in the presence of 1mM extracellular $CaCl_2$ or 2mM EGTA. Traces of Ca^{2+} mobilization are representative of three different experiments (A). Histograms show the quantification of the intracellular concentration of Ca^{2+} 4 minutes after stimulation (grey bar: 1mM extracellular $CaCl_2$; white bar: 2mM EGTA) (B). C) Fura-2AM loaded platelets were stimulated with 20μM $A\beta_{25-35}$ in the presence of 1mM extracellular $CaCl_2$. Where indicated platelets were preincubated with 20 μM Y27632 or 2U/ml apyrase for 10 minutes. Histograms show the quantification of the intracellular concentration of Ca^{2+} 4 minutes after stimulation. Statistical analysis was performed by one-way ANOVA with Bonferroni post-test, n=3, *: $p<0.05$, ***: $p<0.001$, and it is referred to unstimulated sample

Figure 2. $A\beta_{25-35}$ induces dose-dependent α- and dense granule secretion

Flow cytometry analysis of P-selectin exposure in platelets stimulated with the indicated concentrations of $A\beta_{25-35}$ (μM) is shown in (A). Data are expressed as percent of positive cells, and are the mean ± SEM of 4 experiments. Concentration-response analysis of $A\beta_{25-35}$ -induced release of [^{14}C]serotonin from washed human platelets, in the presence (1mM $CaCl_2$. black bar) or in the absence (2mM EGTA: white bar) of extracellular Ca^{2+} (B). The release of serotonin in the supernatant is expressed as percentage of the total incorporated radioactivity upon subtraction of the values measured in the supernatant of resting platelets. Data are expressed as mean ± SEM of three to five different experiments. Statistical analysis was performed by t-test, *: $p< 0.05$, **: $p<0.01$.

Figure 3. $A\beta_{25-35}$-induced signaling pathway activation requires ADP release

Washed platelets (5×10^8/ml, 0.1ml) were treated with 10 μM $A\beta_{25-35}$ for the indicated time (A, B and D) or 2 minutes (C). Where indicated platelets were incubated with 2U/ml apyrase grade VII (apyrase) or buffer (none) for 10 minutes at 37°C prior the addition of $A\beta_{25-35}$. Total proteins were separated by SDS-PAGE and protein phosphorylation was analyzed by immunoblotting with the indicated antibodies: A) anti-P-Akt; anti-PKC phospho-substrates (P-pleckstrin); anti-P-ERK1/2 , anti-P-p38MAPK, and anti-tubulin for equal loading; B) anti-P-Tyr (4G10), D) anti-P-MLC and anti-tubulin for equal loading. In C), washed platelets (1×10^9/ml) treated as described above were lysed and Syk was immunoprecipitated using a specific antibody. Phosphorylation of immunoprecipitated Syk was evaluated with antibody anti-P-tyrosine 4G10. The level of immunoprecipitated protein was confirmed by immunoblotting with anti-Syk antibody. Data shown here are representative of three independent experiments.

Figure 4. $A\beta_{25-35}$ induces integrin αIIbβ3 activation and fibrinogen-binding

Washed platelets (2×10^7/ml, 0.05ml) were treated with Tyrode's buffer (none) or 20μM $A\beta_{25-35}$. FITC-conjugated fibrinogen (5μl) was added to the platelet suspensions and incubated for 30 minutes before dilution with 0.45ml of HEPES buffer. Fibrinogen binding was quantified by flow cytometry. Representative dot plots of the fluorescent labelling (FL1-H: FBN FITC) over forward scattering (FSC) are shown in A). In B), the percentage of fibrinogen positive human platelets stimulated with the indicated concentrations of $A\beta_{25-35}$ are presented. Data are expressed as mean ± SEM of three different experiments.

Figure 5. $A\beta_{25-35}$ induces Rap1b activation dependently on ADP release

Rap1b activation (Rap1b-GTP) was evaluated by activation state-dependent pull-down assay (GST–RalGDSRBD) followed by immunoblotting with anti-Rap1b antibody. Washed platelets were stimulated with different concentrations of $A\beta_{25-35}$ as indicated for 2 minutes (A), or with 10 μM $A\beta_{25-35}$ for the different time (B) or with 10 μM $A\beta_{25-35}$ for 2 minutes (C). In C), platelets were preatreated for 10 minutes with 2U/ml apyrase, 10μM RGDS, or HEPES buffer (none) before stimulation with $A\beta_{25-35}$. Platelets were then lysed, and 0.5 ml of lysates were incubated with GST–RalGDSRBD. The levels of active precipitated Rap1b were tested by immunoblotting (Rap1b-GTP). Upper panels

represent the immunoblot of the pull-down samples. Lower panels show the amount of the total protein (Rap1b). Data shown here are representative of three independent experiments.

Figure 6. $A\beta_{25-35}$-induced platelet aggregation depends on Ca^{2+} mobilization and ADP release

Human washed platelets (3×10^8/ml) were stimulated with different concentrations of $A\beta_{25-35}$ (as indicated) in the presence of 1mM extracellular Ca^{2+} (A, B and C). In B), platelets were also tested in the absence of extracellular Ca^{2+} (none) or preincubated for 2 minutes with 30μM BAPTA. In C) platelets were preincubated for 10 minutes with 2U/ml apyrase. Aggregation was monitored as increase of light transmission up to 5 minutes. Traces in the figure are representative of 3 or more independent experiments. In D) flow cytometry analysis of P-selectin exposure in platelets stimulated with 10 μM $A\beta_{25-35}$ preincubated with 2U/ml apyrase (apyrase: white bar) or buffer (none: grey bar) is shown. In E) $A\beta_{25-35}$ -induced release of [^{14}C]serotonin from washed human platelets, in the presence (white bar) or in the absence (grey bar) of 2U/ml apyrase is shown. The release of serotonin in the supernatant is expressed as percentage of the total incorporated radioactivity upon subtraction of the values measured in the supernatant of resting platelets. For both D) and E), data are expressed as percent of positive cells, and are the mean ± SEM of 3 experiments.

Figure 7. $A\beta_{25-35}$ increases thrombus formation in whole blood under physiological flow conditions in an ADP-dependent manner

Human platelet-rich plasma (PRP) was isolated from anticoagulated blood (citrate) and incubated for 1 hour with Calcein AM (5 μg/ml) at 37°C. After reconstitution of whole blood by mixing labelled PRP and the red blood cell fraction, thrombus formation was monitored under physiological shear stress conditions (1000 sec^{-1}). Coating of the microvessel was performed for 60 minutes at 37C with collagen alone (1mg/ml) or collagen plus $A\beta_{25-35}$ (20 μM) (A and B). Where indicated, apyrase (1U/ml) was added to the blood 10 minutes prior the assay (B). Both panels show a representative picture of the thrombi and a quantification of the surface coverage after 10 minutes of flow (mean ± SEM, n=4). Statistical significance of the differences was measured using a t-test for paired samples (* = $p<0.05$).

Figure 8. A model for $A\beta_{25-35}$-induced platelet activation

In the presence of extracellular Ca^{2+}, $A\beta_{25-35}$ promotes mobilization of intracellular Ca^{2+}, initial phosphorylation of MLC and consequent release of dense granules, with secretion of ADP. ADP in turn activates platelets through several intracellular protein kinase pathways, including tyrosine kinases (Tyr-K), Syk, PI3K, PKC, ERK1/2 and p38MAPK. Resulting activation of Rap1b and integrin $\alpha_{IIb}\beta_3$ leads to platelet aggregation and thrombus formation.

figure 1

A

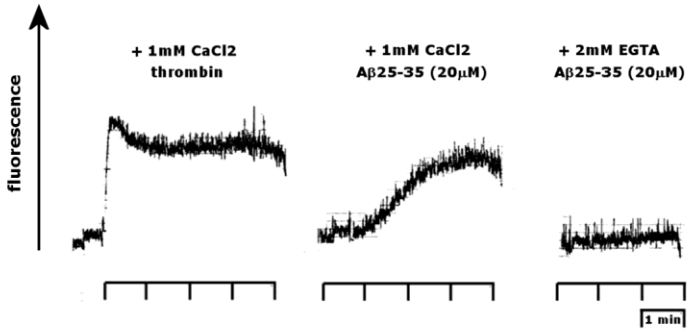
fluorescence
+ 1mM CaCl2
thrombin
+ 1mM CaCl2
Aβ25-35 (20μM)
+ 2mM EGTA
Aβ25-35 (20μM)
1 min

B

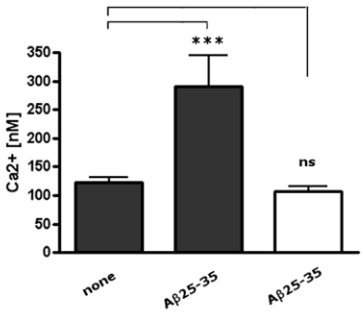
Ca2+ [nM]
350
300
250
200
150
100
50
0
***
ns
none
Aβ25-35
Aβ25-35

C

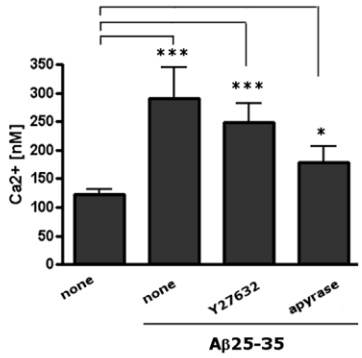
Ca2+ [nM]
350
300
250
200
150
100
50
0
***
***
*
none
none
Y27632
apyrase
Aβ25-35

figure 2

A

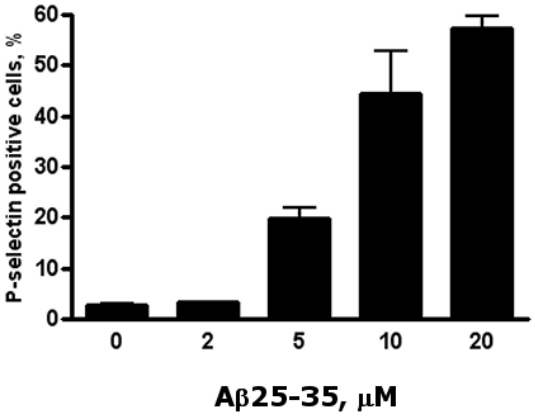
P-selectin positive cells, %
60
50
40
30
20
10
0
0
2
5
10
20
Aβ25-35, μM

B

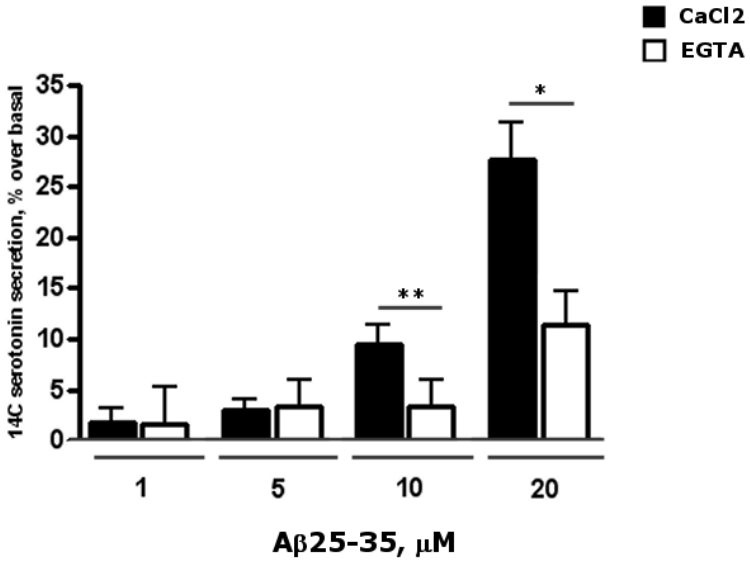
CaCl2
EGTA
14C serotonin secretion, % over basal
35
30
25
20
15
10
5
0
**
*
1
5
10
20
Aβ25-35, μM

figure 3

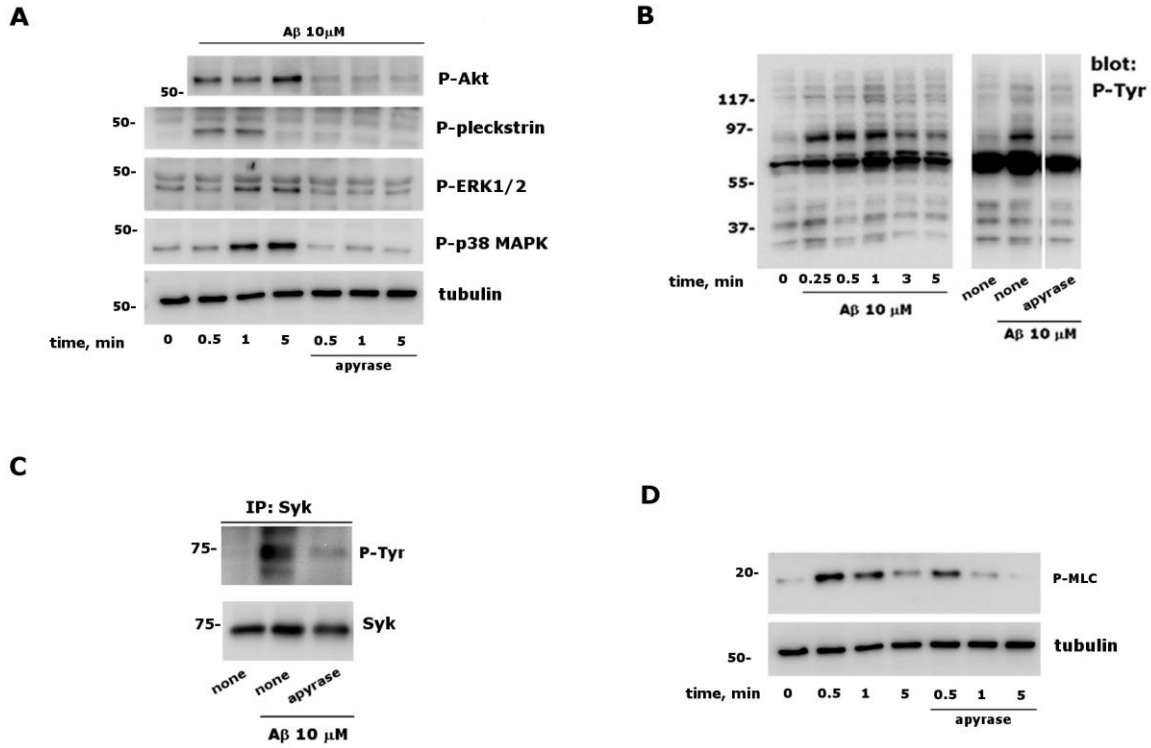
A
Aβ 10μM
P-Akt
P-pleckstrin
P-ERK1/2
P-p38 MAPK
tubulin
50-
time, min
0 0.5 1 5 0.5 1 5
apyrase
B
blot:
P-Tyr
117-
97-
55-
37-
time, min
0 0.25 0.5 1 3 5
Aβ 10 μM
none none apyrase
Aβ 10 μM
C
IP: Syk
75-
P-Tyr
Syk
none none apyrase
Aβ 10 μM
D
20-
P-MLC
50-
tubulin
time, min
0 0.5 1 5 0.5 1 5
apyrase

figure 4

A

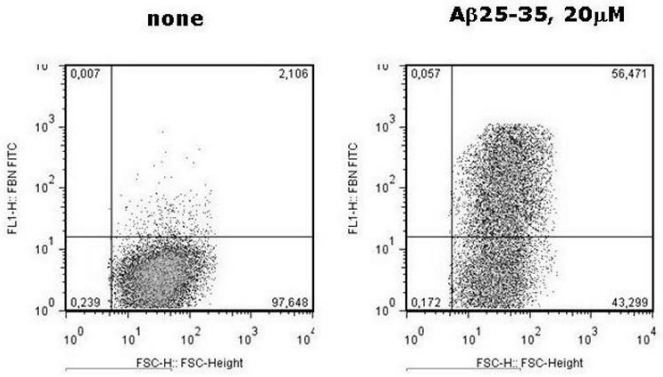
none
Aβ25-35, 20μM
0,007
2,106
0,239
97,648
0,057
56,471
0,172
43,299
FL1-H:: FBN FITC
FSC-H:: FSC-Height

B

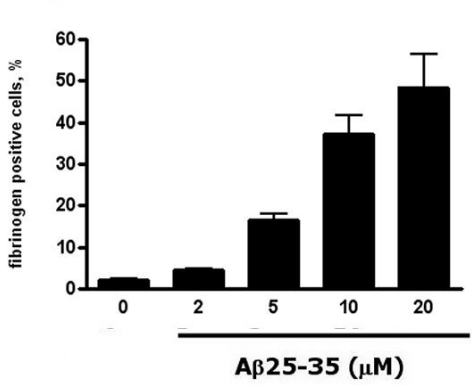
fibrinogen positive cells, %
0
10
20
30
40
50
60
0
2
5
10
20
Aβ25-35 (μM)

figure 5

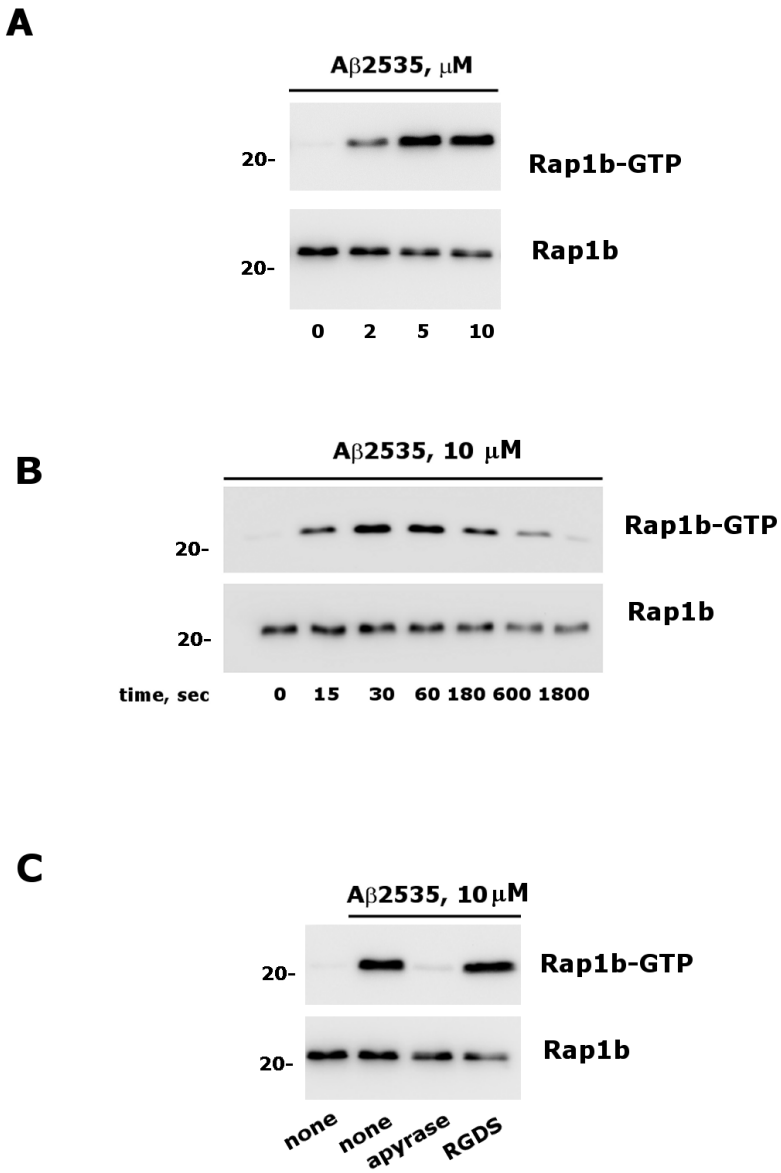
A
Aβ2535, μM
20-
Rap1b-GTP
20-
Rap1b
0 2 5 10
B
Aβ2535, 10 μM
20-
Rap1b-GTP
20-
Rap1b
time, sec
0 15 30 60 180 600 1800
C
Aβ2535, 10μM
20-
Rap1b-GTP
20-
Rap1b
none
none
apyrase
RGDS

figure 6

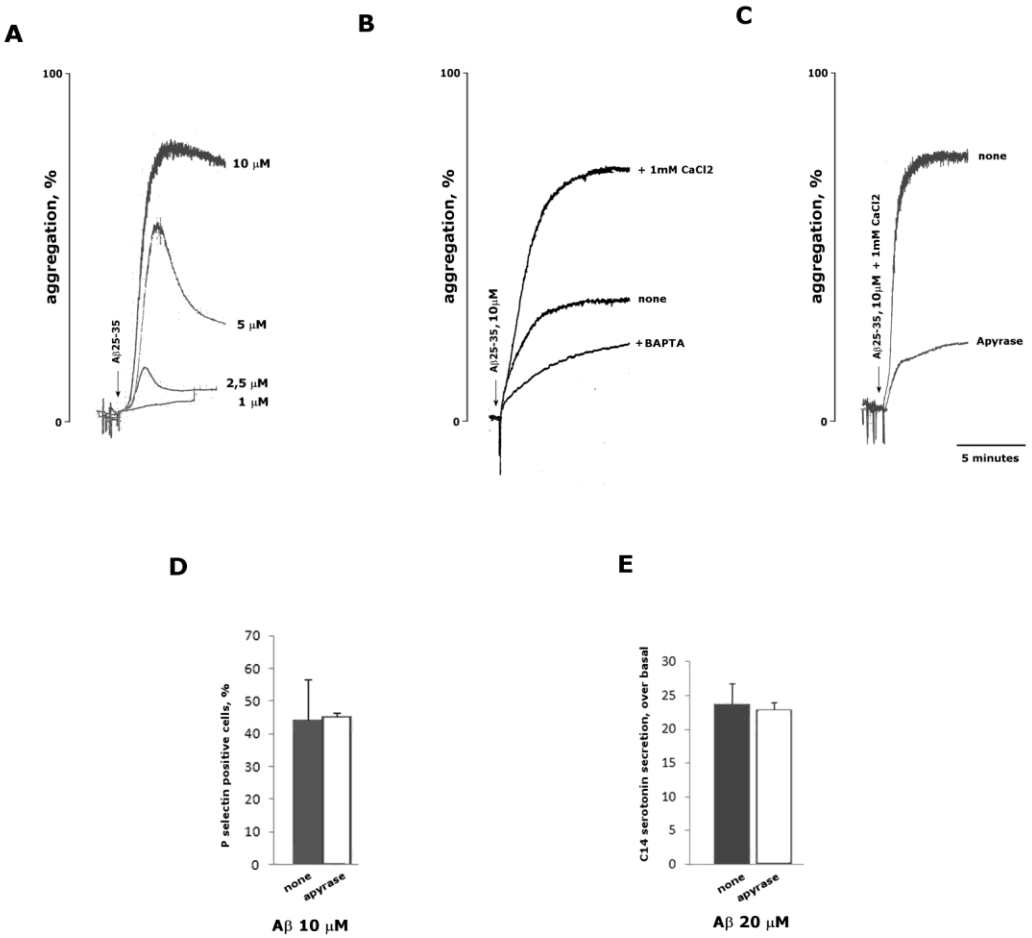
A
B
C
100
0
aggregation, %
Aβ25-35
10 μM
5 μM
2,5 μM
1 μM
Aβ25-35, 10μM
+ 1mM CaCl2
none
+BAPTA
Aβ25-35, 10μM + 1mM CaCl2
Apyrase
5 minutes
D
E
P selectin positive cells, %
70
60
50
40
30
20
10
0
none
apyrase
Aβ 10 μM
C14 serotonin secretion, over basal
30
25
20
15
10
5
0
Aβ 20 μM

Figure 7

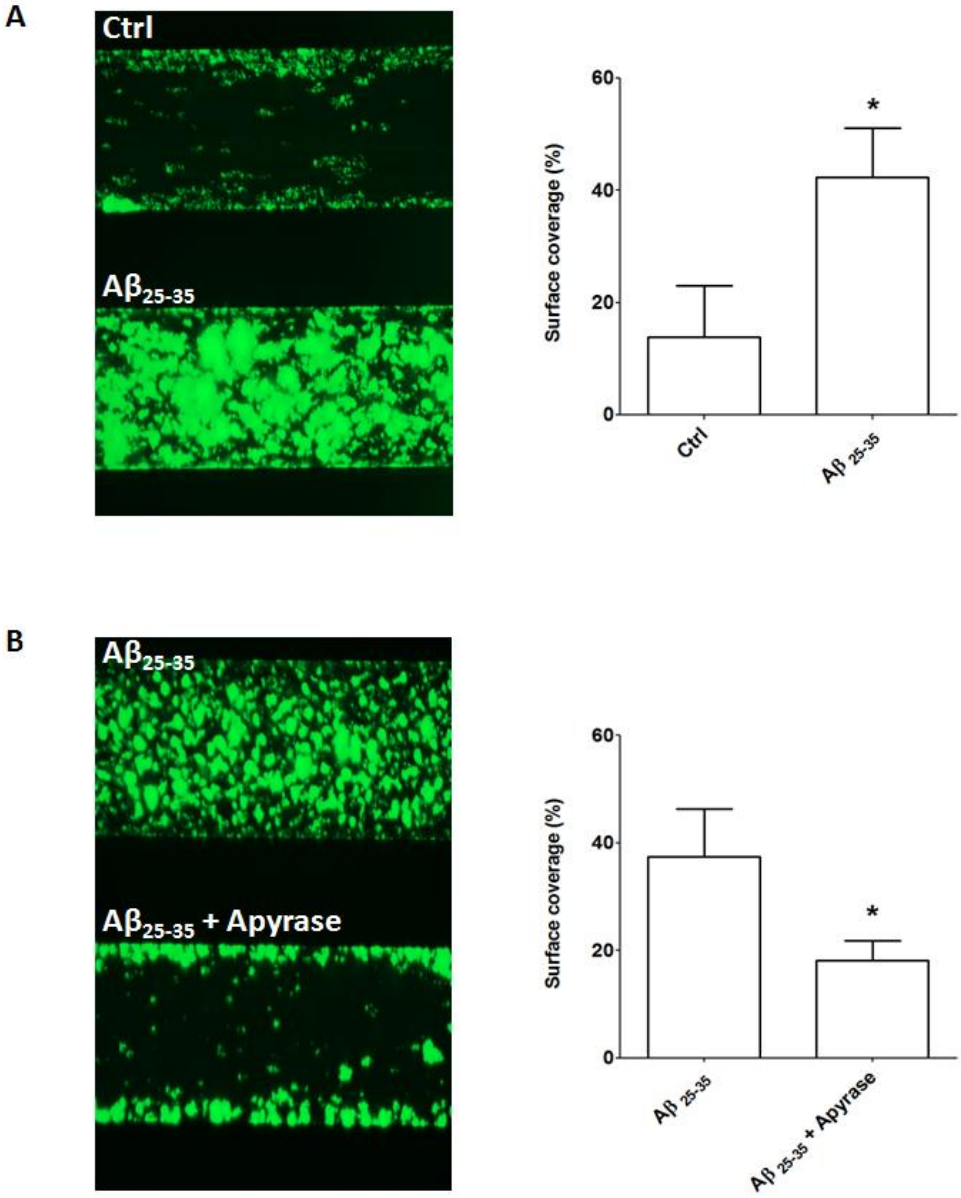
A
Ctrl
Aβ25-35
Surface coverage (%)
60
40
20
0
*
Ctrl
Aβ 25-35
B
Aβ25-35
Aβ25-35 + Apyrase
Surface coverage (%)
60
40
20
0
*
Aβ 25-35
Aβ 25-35 + Apyrase

Figure 8

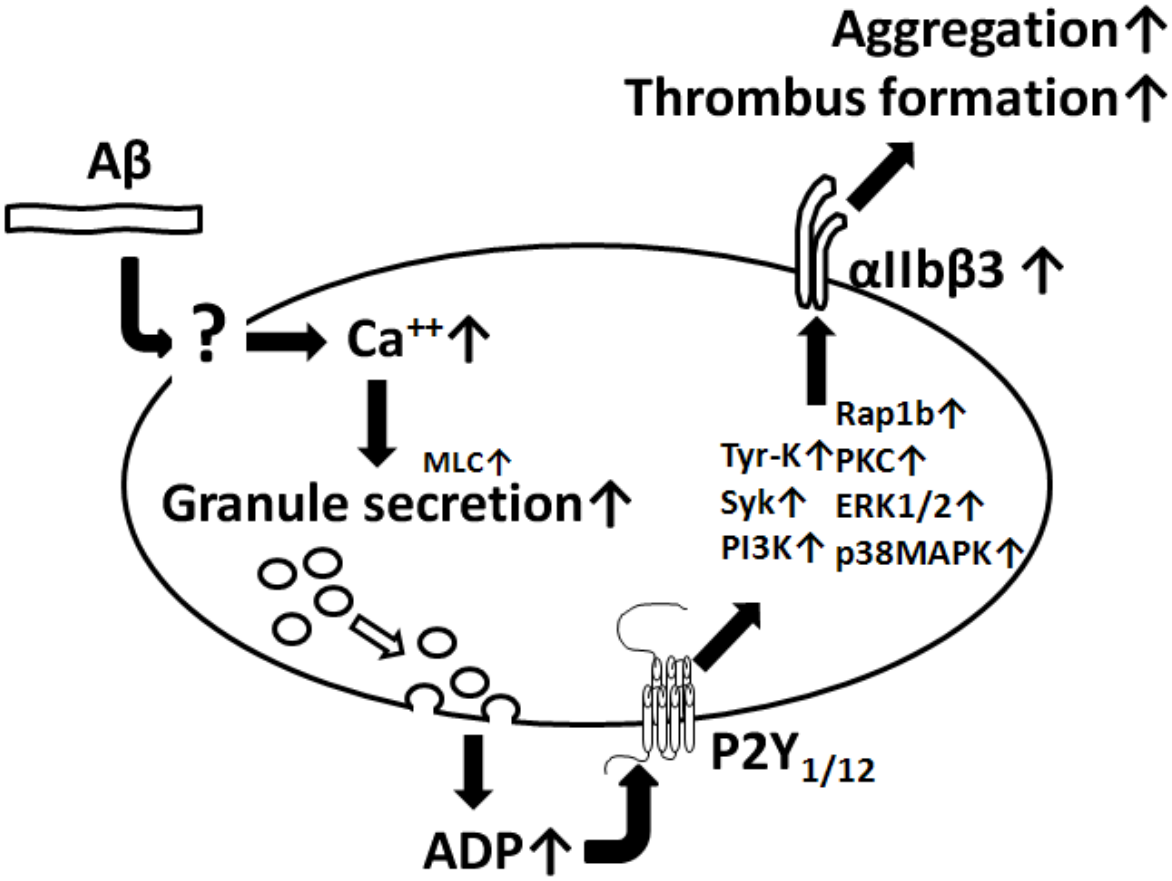
Aggregation↑
Thrombus formation↑
Aβ
?
Ca++↑
αIIbβ3 ↑
MLC↑
Granule secretion↑
Rap1b↑
Tyr-K↑ PKC↑
Syk↑ ERK1/2↑
PI3K↑ p38MAPK↑
P2Y1/12
ADP↑